Available online at www.sciencedirect.com
ScienceDirect
Ceramics International 37 (2011) 2997–3004
CERAMICS INTERNATIONAL
www.elsevier.com/locate/ceramint

Enhancement in dielectric and ferroelectric properties of lead free $Bi_{0.5}(Na_{0.5}K_{0.5})_{0.5}TiO_3$ ceramics by Sb-doping

Krishan Kumar [a], B.K. Singh [a], M.K. Gupta [a], N. Sinha [b], Binay Kumar [a,*]

[a] Crystal Lab, Department of Physics & Astrophysics, University of Delhi, Delhi 7, India
[b] Department of Electronics, SGTB Khalsa College, University of Delhi, Delhi 7, India

Received 11 January 2011; received in revised form 8 April 2011; accepted 11 April 2011
Available online 15 April 2011

Abstract

Lead free piezoelectric $Bi_{0.5}(Na_{0.5}K_{0.5})_{0.5}TiO_3$ (pure and 1 wt.%, 2 wt.%, 4 wt.% Sb-doped) ceramics were synthesized away from its MPB. The crystalline nature of the BNKT ceramic was studied by XRD and SEM. Depolarization temperature (T_d) and transition temperature (T_c) were observed through phase transitions in dielectric studies which were found to increase after Sb-doping, thus increasing its usable temperature range. In the study of relaxation behavior, the activation energy for relaxation was found to be 0.33, 0.43, 0.57 and 0.56 eV for pure and Sb-doped samples, respectively. All samples were found to exhibit normal Curie–Weiss law above their T_c. Doping of Sb was found to restrain the diffused character of the pure sample. In *P–E* loop, Sb-doping was found to increase the ferroelectric properties.

Pure and Sb-doped BNKT ceramics exhibited high values of piezoelectric charge coefficient (d_{33}) as 115, 121, 129 and 100 pC/N, respectively.

Keywords: A. Sintering; C. Dielectric properties; C. Ferroelectric properties; D. Perovskites

1. Introduction

Lead based PT and PZT ceramics are widely used in piezoelectric sensors, transducers and actuators applications [1–4]. However, due to the presence of lead, which is a very hazardous material, the attention is attracted towards the class of ferroelectric materials which do not contain lead but still have very good dielectric and ferroelectric properties. Lead free sodium bismuth titanate (NBT: $Na_{0.5}Bi_{0.5}TiO_3$) based ceramic is one of the promising candidate having good dielectric and ferroelectric properties [5–7], along with a high Curie temperature ($T_c \sim 320\ ^\circ C$), remnant polarization ($P_r \sim 38\ \mu C/cm^2$) and conductivity [5]. However, its usable temperature range is restricted to approximately 200 °C as its piezoelectric property disappears above this temperature. This is due to the presence of anomaly in its dielectric properties as a result of low-temperature phase transition from ferroelectric to anti-ferroelectric phase and hence reducing its suitability for various industrial applications. This transition temperature is called depolarization temperature (T_d) and its high values are a necessity for wider applications. Consequently, many attempts have been made to enhance the piezoelectric and dielectric properties of NBT by various ionic substitutions at *A* or *B* site [8–10]. However, these substitutions/doping have been observed to further reduce its T_d-value. Potassium bismuth titanate (KBT: $K_{0.5}Bi_{0.5}TiO_3$) is a ferroelectric material with a relatively higher curie temperature (~380 °C) than that of NBT which shows a second order phase transition from the tetragonal phase to the pseudocubic phase. Due to a relatively higher T_d for KBT (250–340 °C) than that of NBT, a binary system of KBT and NBT was expected to possess a high T_d value. The low density lead free alkali based materials would also be at advantage in transducer for underwater and medical imaging due to expected lower acoustical impedance. However, a complex system of NBT and KBT (BNKT), having very high T_c and reasonably good piezoelectric properties near its morphotropic phase boundary (MPB), as compared to other lead free piezoelectric ceramics, did not show any substantial increase in the T_d [11]. Further, a high coercive field ($E_c \sim 80$ kV/cm) causes problem in the poling process [10]. The system BNKT is generally expressed as formula

* Corresponding author. Fax: +91 011 27667061.
E-mail addresses: b3kumar69@yahoo.co.in, bkumar@physics.du.ac.in (B. Kumar).

0272-8842/$36.00
doi:10.1016/j.ceramint.2011.04.013

$(1-x)$NBT $-$ xKBT and its MPB lies in the range of $0.16 \leq x \leq 0.20$ [12]. However, very few reports are available for this material synthesized away from its MPB till date [13,14] and these are mostly confined to ferroelectric and piezoelectric characterizations. There have been some reports on the effects of [Li, Nd, Ce] doping on BNKT system in which T_d has been found to decrease [8–10]. In the present paper, synthesis and investigation of pure and Sb-doped BNKT ceramic for its structural and dielectric behavior has been undertaken for BNKT50 ($x = 0.5$) ceramic away form its MPB, with an aim to increase the T_d-value. Further, an investigation on the optimization of Sb-doping concentration has been undertaken so as to exhibit better piezoelectric and dielectric properties. The results have been analyzed in detail.

2. Experimental procedure

High purity Bi_2O_3, K_2CO_3, Na_2CO_3, TiO_2, and Sb_2O_3 (purity > 99% Sigma–Aldrich) were used as starting materials. The raw materials were weighed according to the composition $Bi_{0.5}(Na_{1-x}K_x)_{0.5}$ TiO_3 ($x = 0.5$) (BNKT50). The pure and Sb-doped (1 wt.%, 2 wt.%, 4 wt.%) BNKT (here after termed as samples *A*, *B*, *C* and *D*, respectively) were mixed by using ball mill for 10 h with a ball to powder ratio 2:1. Then the dried powder was calcined at 900 °C for 4 h. After calcinations, powders were reground and mixed with binder (polyvinyl alcohol). After drying, pellets of 12 mm diameter and 1.5 mm thickness were prepared by applying 250 MPa of pressure using hydraulic press. The pellets of the different samples were kept at 600 °C to burn the binder. Each sample was sintered at different temperatures viz. 1000, 1025, 1050, 1075 and 1100 °C for 4 h in each case to study the effect of the Sb-doping on the sintering temperature and hence to obtain the optimized sintering temperature. The samples were sintered at their optimum sintering temperature. The obtained ceramic were finely grounded and subjected to powder XRD in the range 20–70° of 2θ with a step angle of 0.02° and step time 0.2 s using PW3710 Philips diffractometer (CuK_α radiation) to confirm the phase formation and crystalline nature. After polishing and electroding, the samples were subjected to various characterizations. The variation of dielectric constant with temperature at different frequency (100 Hz–2 MHz) was studied from room temperature to 550 °C using an Agilent E4980A impedance analyzer. The Hysteresis loop was traced by using computer controlled *P–E* loop tracer. Ceramics were poled by applying a field of 20 kV/cm at 70 °C for 1 h. The piezoelectric charge coefficient d_{33} (pC/N) was measured using Piezometer (PM300, Piezotest). Surface morphology/microstructure of the sintered pellets at room temperature was examined by a scanning electron microscopy (ZEISS-MA10, SEM). The pellets were gold coated for SEM study. The results were analyzed and discussed in detail.

3. Results and discussion

The samples are prepared after sintering the pellets at different temperatures. The optimum sintering temperature

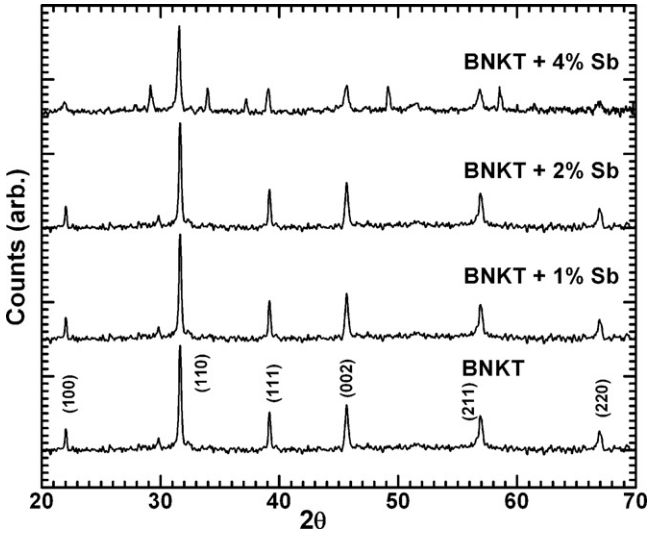

Fig. 1. X-ray diffraction pattern of BNKT and Sb-doped BNKT ceramic.

obtained for samples *A* and *B* was found to be in the range of 1025–1050 °C while for higher concentration of Sb (samples *C* and *D*), it was found to be in the range of 1075–1100 displaying that the optimum sintering temperature increases with Sb concentration in the sample. The XRD patterns of optimally sintered samples are shown in Fig. 1. All patterns exhibit a single perovskite phase. This conveys that doping ions completely diffused into BNKT lattice up to a doping concentration of 2%. However, some additional peaks in the diffraction pattern for sample *D* shows the distortion in the lattice arrangement due to excess doping of Sb^{3+} (4%). The room temperature XRD data for all samples were analyzed using X' Pert High Score Plus and Check Cell software for calculating lattice parameters and refining the obtained cell parameters, respectively. The obtained lattice parameters are found to be in good agreement with the earlier reported values for BNKT50 single crystal [15].

Surface property and microstructure were studied through scanning electron micrographs of the sintered samples at room temperature (Fig. 2). The micrographs show the cross-section morphological features of BNKT + Sb-doped (1 wt.%, 2 wt.%, 4 wt.%) ceramics as revealed by the scanning electron microscope (SEM). Results have confirmed the formation of single phase compound. It is clear from the figures that the surface of all samples is homogeneous. The grains are found to be uniformly distributed showing the homogeneity on the surface of all samples. The grains are observed to be of almost regular in shape for samples '*A*', '*B*' and '*C*' ceramic but in the case of sample '*D*' they are found to be irregular in shape. The grain boundaries can be clearly observed in all samples. The average grain size for samples *A*, *B*, *C* and *D* were discovered to be 1, 3, 5, 2 μm across, respectively, implying that the crystallite size was increasing with the doping concentration. The decrease in grain size in sample *D* may be attributed to the segregation of Sb^{3+} ion at the grain boundaries that prevented the grain boundary movement during the sintering and inhibited the grain growth. XRD results portrayed the same conclusion by the presence of some additional peak. The SEM images

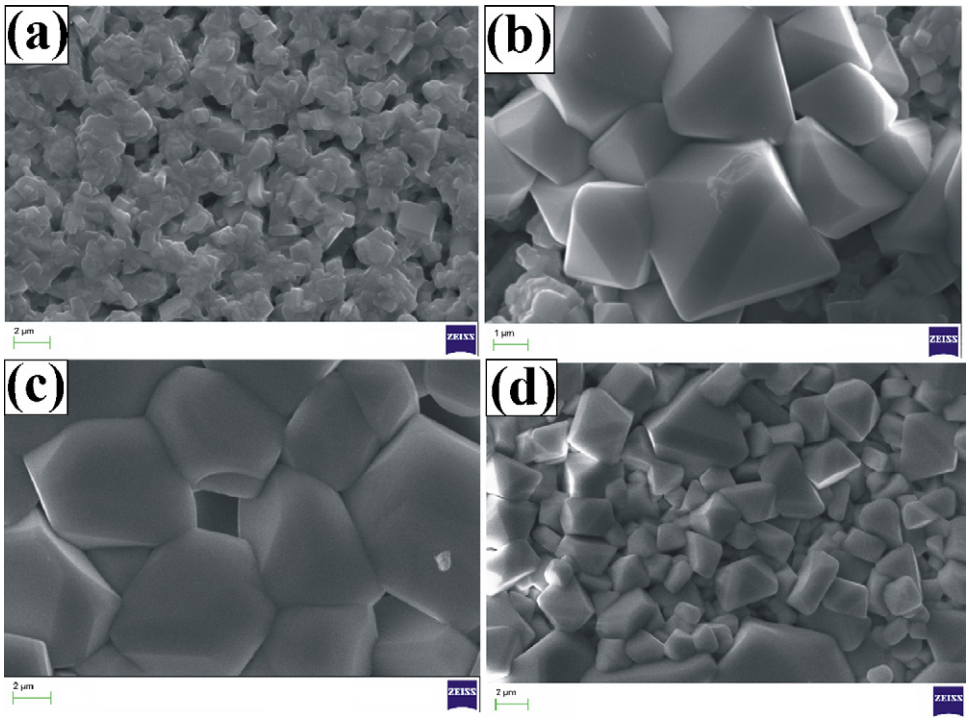

Fig. 2. Scanning electron micrograph of pure and 1%, 2% and 4% Sb-doped BNKT.

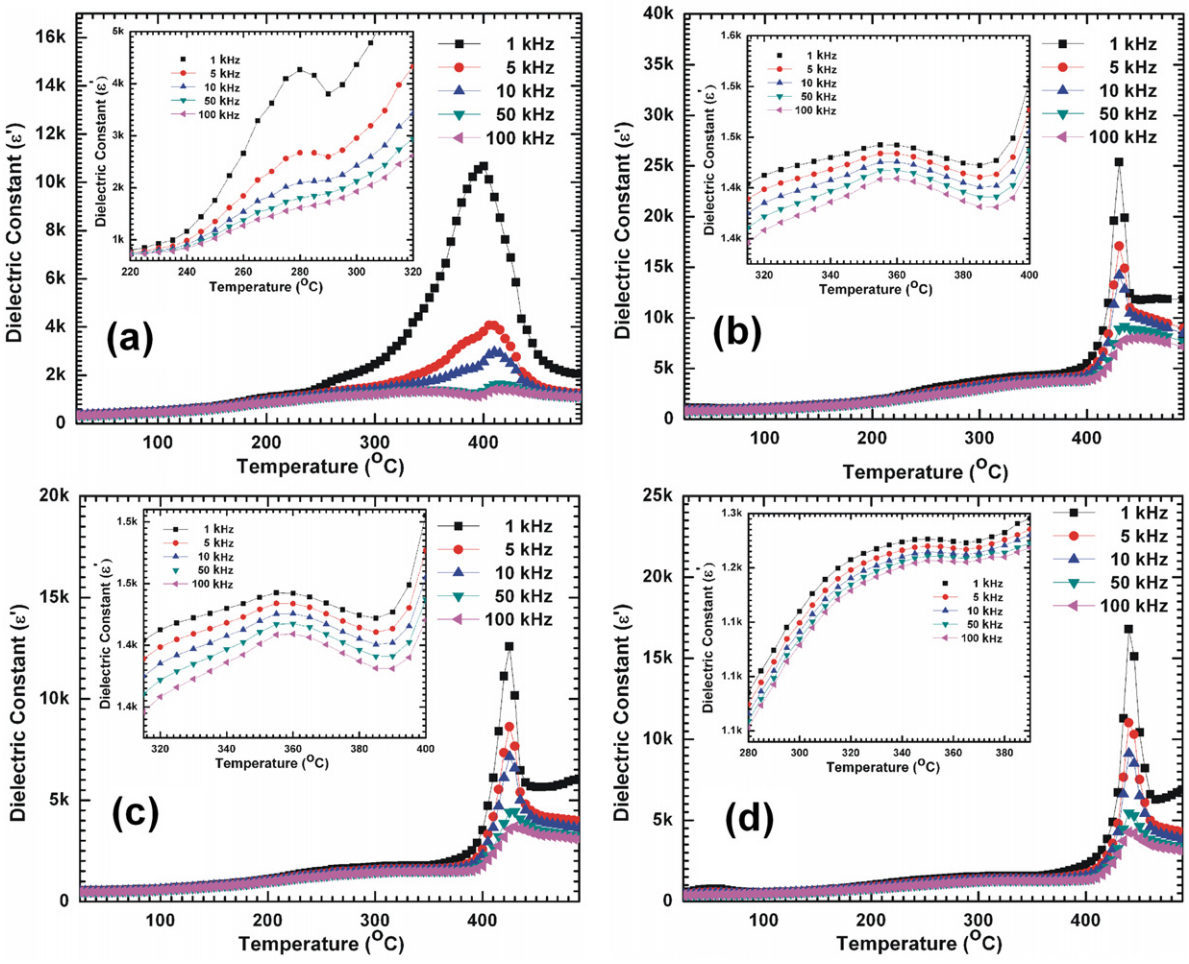

Fig. 3. Variation of real part of dielectric constant (ε') with temperature (the inset shows the T_d of pure and doped BNKT ceramic).

confirmed that the Sb-doped BNKT ceramics are denser than pure BNKT ceramic.

Dielectric studies of the as grown unpoled pure and Sb-doped BNKT ceramic were carried out to analyze its response to an applied low ac voltage (1 V). The variation of real part of dielectric constant (ε') with temperature at various frequencies for samples *A*, *B*, *C* and *D* are as shown in Fig. 3a, b, c and d, respectively. A relatively higher dielectric constant (∼10*k*) near its T_c (∼395 °C) is observed for sample *A* when compared with earlier reports (∼5*k*) for BNKT ceramic synthesized near its MPB [14]. However, these values for pure and Sb-doped ceramic away from its MPB ($x = 0.5$) have been reported for the first time. The increase in the dielectric constant (ε') of all samples with temperature is due to the space charge polarization. Additionally, an increase in the dielectric constant (∼25,000) is observed when 1% Sb is doped. Further increase in the doping concentration has resulted in the decreased value of ε' (∼16*k* and 13*k* for 2% and 4% Sb-doped, respectively). This demonstrates that the optimum doping concentration for obtaining a higher dielectric constant is within the range 1–2%.

Here, the first dielectric peak T_d (depolarization temperature) corresponds to the change from ferroelectric phase to anti ferroelectric phase while T_c corresponds to a change from anti-ferroelectric phase to paraelectric phase. Both T_d and T_c are found to be frequency dependent only for sample *A* i.e. a shift towards high temperature is observed with the increase in frequency. On the other hand, Sb-doped samples do not exhibit frequency dependence for T_d and T_c. However, changes in the T_d and T_c values are observed as a function of doping concentration which is similar to the variation observed for dielectric constant as shown in Fig. 4. T_d and T_c are detected to increase with doping concentration and attain the highest value of T_d (∼355 °C) for sample *C*. Further increase in doping concentration tends to decrease its T_d and T_c values. It is evident from the curve that the optimum Sb-doping in order to increase its T_d, which makes it more suitable for various industrial applications at an elevated temperature, is in the range of 1–2%. It is to be mentioned here that the phase transition for the present system is due to Na^+, K^+ and Bi^{3+} ions distributed randomly at the *A*-site. The occupancy of *A*-site by Na^+, K^+ and Bi^{3+} ions induces a relaxor ferroelectric behavior in pure BNKT based ceramic. The most of the Sb^{3+} (0.76 Å) ions were likely to enter at *A*-site due to small ionic radii of Sb^{3+} (0.76 Å) than that of Bi^{3+} (1.03 Å), K^+ (1.38 Å) and Na^+ (1.02 Å). In the present case Sb^{3+} ions act as a donor and create the cation vacancies in BNKT ceramics, which reduce the oxygen vacancies. These oxygen vacancies are the main cause of domain wall clamping [16]. Finally, the reduction of domain wall clamping results in an increase in dielectric constant. Further, to some extent, this clamping will restrain the macro–micro domain sintering and ferroelectric to anti ferroelectric phase transition, which eventually be the reason for more variation in T_d [17].

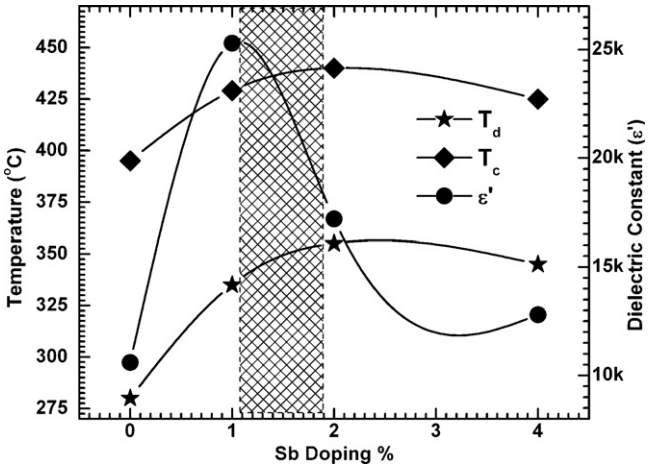

Fig. 4. Variation of T_d and T_c with Sb-doping concentration.

The ferroelectric properties of these ceramics strongly depend on three factors, viz doping concentration, diffusion of doping ions into *A*- or *B*-site and grain/particle size. As discussed before, these dopants occupy the *A*- or *B*-site randomly in the sub-lattice of ABO_3 perovskite unit. A number of chemical micro regions with distinctive composition of the *A*- or *B*-site cations are formed. Each of these micro region possesses its own transition temperature, and hence leads to relaxor characteristic [18,19]. Fig. 5a, b, c, d show the variation of relaxation time $\ln(\tau)$ with $1/k_BT$ for samples *A*, *B*, *C* and *D*, respectively. The relaxation time (τ) is calculated from the temperature of dielectric maxima for different frequencies. The variation of the relaxation time with temperature is given by the Arrhenius equation

$$\tau = \tau_o e^{(-E_{relax}/k_BT)}$$

where E_{relax} is the activation energy for relaxation and k_B is the Boltzmann's constant. It can be seen that typical variation of the relaxation time shows a steady increase with a gradual change of slope in the different temperature region for all samples. This implies that the electrical relaxation may be due to the migration of charged species/defects ion complexes. The activation energy for relaxation for all samples are calculated by linear fitting of the curve and are found to be 0.33, 0.43, 0.57 and 0.56 eV for samples *A*, *B*, *C* and *D*, respectively. The increase in the activation energy is the main cause of decrease in oxygen vacancies. This shows that the sample *A* is found to show more relaxation behavior as compared to samples *B*, *C* and *D*.

Fig. 6a, b, c and d shows the variation of imaginary part of dielectric constant with frequency at different temperature for *A*, *B*, *C* and *D*, respectively. The imaginary part of dielectric constant was found to decrease sharply up to 5 kHz frequency, after which a constant value for all samples are observed. The frequency dependence of the imaginary part of the dielectric constant is analyzed using power square law given by Jonscher, who suggested that the behavior of dipolar system can be characterized by fractional power laws in frequency above the loss peak frequency as $\varepsilon'' \propto f^{n-1}$ where *n* is an exponent ($0 < n < 1$) [20]. The obtained curve was fitted with above equation and the value of *n* was observed to decrease from 0.88 to 0.35, 0.88 to 0.30, 0.85 to 0.28, 0.76 to 0.26 for samples *A*, *B*, *C* and *D*, respectively, for a temperature variation from 250 to 550 °C.

If a material shows the normal ferroelectric behavior, it follows Curie–Weiss law above T_c as $\varepsilon = C/(T - T_C)$, where *C*

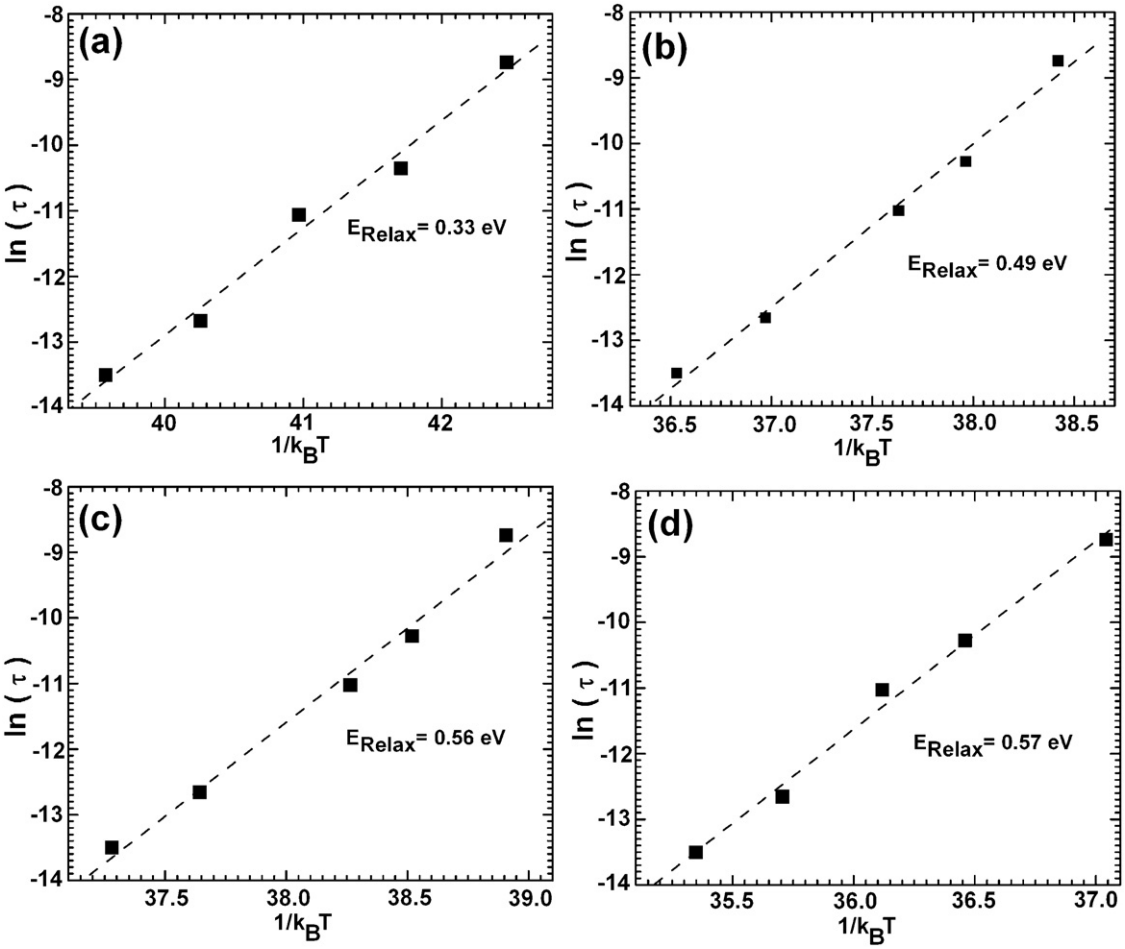

Fig. 5. Plot between the relaxation time (ω) and $1/k_BT$ for (a) pure, (b) 1% Sb-doped, (c) 2% Sb-doped and (d) 4% Sb-doped BNKT ceramic.

is the Curie–Weiss constant and T_c is the Curie–Weiss temperature [21]. Fig. 7 shows the variation of Curie constant at 1 kHz for all samples as a function of temperature above T_c. The linear fitting of all the data was found to be almost linear confirming that all the samples follow Curie–Weiss law and hence they all are normal ferroelectric.

The diffused phase transition is observed only in the case of sample *A*, as exemplified by broadening of dielectric peak (Fig. 2a). Therefore, the nature of diffusivity is studied only for this sample. Fig. 8 shows the plot of $\log((1/\varepsilon') - (1/\varepsilon'_m))$ vs $\log(T - T_m)$ at different frequencies for sample *A*. The equation $1/\varepsilon = (T - T_m)^2$ has been proven to be valid over a wide temperature range instead of the normal Curie–Weiss law, where T_m is the temperature at which the dielectric constant is the maximum. For the explanation of dielectric behavior of complex ferroelectrics with diffuse phase transition, Curie temperature distribution is Gaussian where the reciprocal permittivity can be written as [22]:

$$\frac{1}{\varepsilon} = \frac{1}{\varepsilon_m} + \frac{(T - T_m)^\gamma}{2\varepsilon_m \delta^2}$$

where ε_m is maximum dielectric constant, γ is the diffusivity for phase transition (which is the expression of the degree of dielectric relaxation) and δ is diffuseness parameter (used to measure the degree of diffuseness of the phase transition). If the value of γ is 1 then the material belongs to normal ferroelectric and if $\gamma = 2$, material belong to ideal relaxor ferroelectric. The values of γ and δ are both material constants which depend on the composition and structure of the material. After fitting the curve (Fig. 8), the slope of the curve is obtained for different frequencies and the values of γ and δ are calculated. The value of γ is found to vary between 1.67 and 1.92, which confirms the diffuse phase transition in BNKT system. The value of δ is found vary in the range of 23–32.

Fig. 9 shows the electrical polarization vs electric field (*P–E*) for samples *A*, *B*, *C* and *D* at room temperature. From the Hysteresis loop, the values of coercive field (E_c) for the samples *A*, *B*, *C* and *D* were found to be 26, 27, 33 and 28 kV/cm, respectively, while remnant polarizations (P_r) were found to be 33, 26, 38 and 29 $\mu C/cm^2$, respectively. These values of ferroelectric properties are strongly influenced by composition and its homogeneity, defects, external field and orientation of domains, which eventually contribute to the material response. Uniform oriented domain structure actually increases the ferroelectric properties. In the present case, the higher value of P_r for sample *C* shows the presence of more uniform domain structure. Further, a decrease in the P_r for sample *D* with Sb

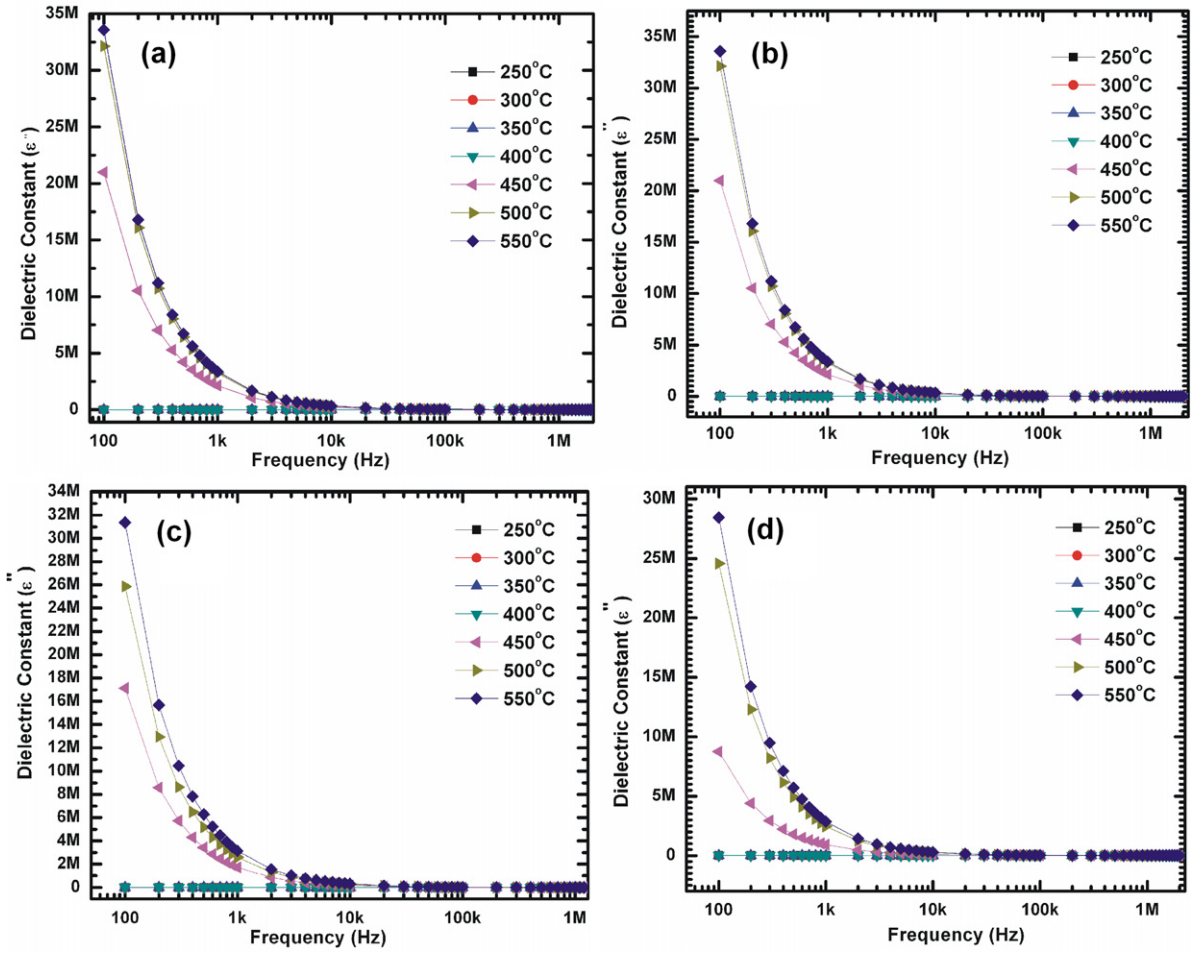

Fig. 6. Imaginary part of dielectric constant vs frequency plots at different temperatures for pure and Sb-doped BNKT ceramic.

doping concentration may be attributed to a non-uniform domain structure and existence of mixed domain [23]. Conclusively, the uniformity of the domain structure is disrupted with the increase in doping percentage.

According to Haertling and Zimmer the empirical relation between remanent polarization, saturation polarization and polarization at fields above coercive field is given by the relation $R_{sq} = (P_r/P_s) + (P_{1.1E_c}/P_r)$ [24], where R_{sq}, P_s and $P_{1.1E_c}$ are the squareness of Hysteresis loop, saturation polarization and polarization at an electric field equal to 1.1 times the coercive field, respectively. For an ideal Hysteresis loop the squareness parameter is equal to 2. Using this relation,

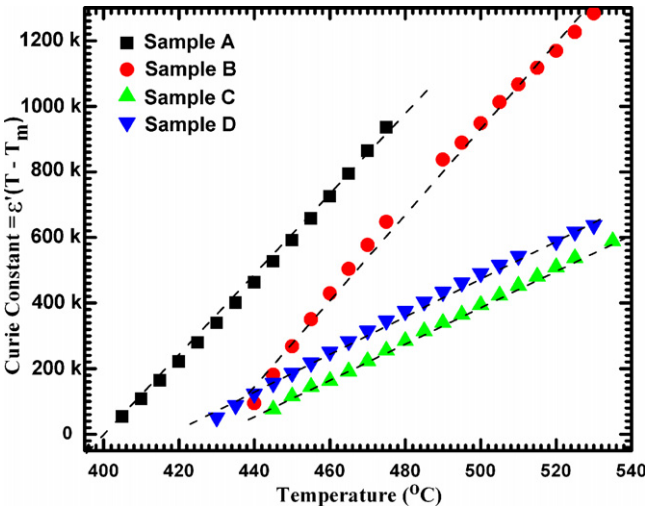

Fig. 7. Variation of Curie constant with temperature at 1 kHz.

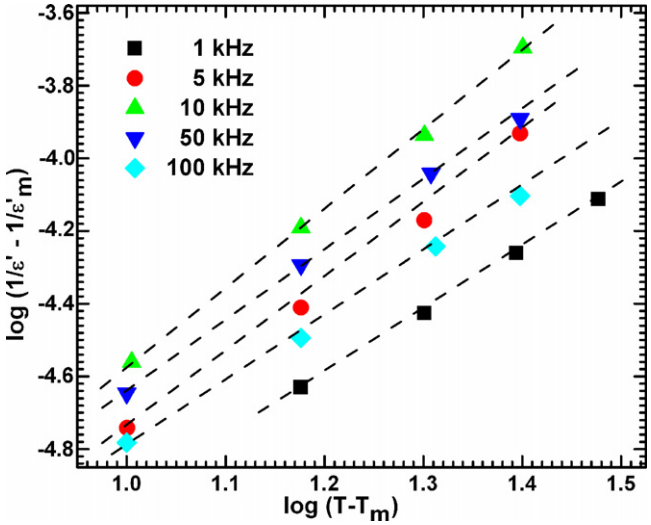

Fig. 8. Plot of $\log((1/\varepsilon') - (1/\varepsilon'_m))$ vs $\log(T - T_m)$, at different frequencies for pure BNKT ceramic.

Table 1
Comparison of various dielectric and piezoelectric/ferroelectric parameters of pure and Sb-doped BNKT ceramic.

Sample name	T_c (°C)	T_d (°C)	ε'	d_{33} (pC/N)	P_r (μC/cm^2)	E_c (kV/cm)	R_{sq}
Pure BNKT (*A*)	395	280	10.6*k*	115	33	26	1.78
1% Sb-doped BNKT (*B*)	430	335	25.3*k*	121	26	27	1.73
2% Sb-doped BNKT (*C*)	450	355	17.2*k*	129	38	33	1.82
4% Sb-doped BNKT (*D*)	425	345	12.8*k*	100	29	28	1.80

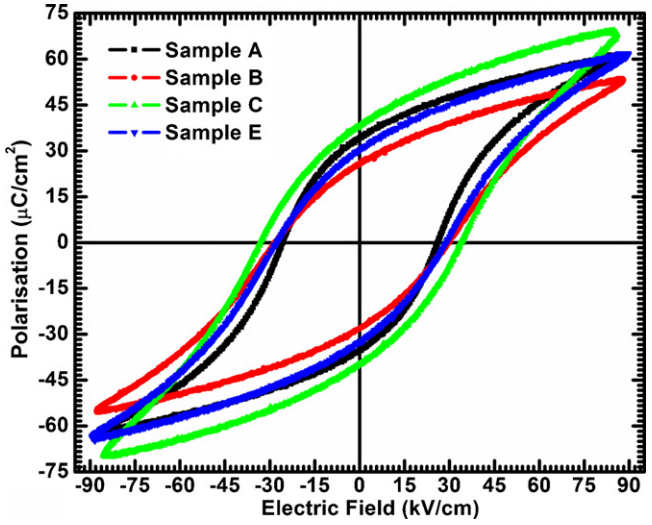

Fig. 9. Hysteresis loop of pure and Sb-doped BNKT ceramic at a maximum field of 38 kV/cm at room temperature.

a quantification of changes in the Hysteresis behavior for each sample can be done. The squareness parameter for all the four loops were calculated and found to be 1.78, 1.73, 1.82 and 1.80, respectively. Further, an increase in the R_{sq} for the samples *A*, *B*, *C* and *D* shows that a better switching behavior of polarization can be achieved with increased Sb concentration.

All the samples were poled at electric field of 2 kV/mm at a temperature of 70 °C for 1 h. The d_{33} value as high as 115, 121, 129 and 100 pC/N were observed for samples *A*, *B*, *C* and *D*, respectively. This shows that Sb-doping in the range of 1–2% significantly enhances the piezoelectric properties of the BNKT ceramic. The Sb-doping disturbs the BNKT lattice structure due to the difference in their ionic radii as discussed in the context of increased dielectric constant. The lattice deformation caused by the substitution of Sb^{3+} ions at *A*-site, which act as donor ions leading to creation of vacancies in *A*-site, can enhance the motion of domains which leads to the improvement of the piezoelectric properties. However, for the sample *D* the segregation along the grain boundaries may restrict the Sb^{3+} ions to take part in this regular substitution and may decrease the value of d_{33}. The various physical, dielectric and piezoelectric properties of all the four samples are compared and shown in Table 1.

4. Conclusion

Sb-doped (1, 2 and 4 wt.%) $Bi_{0.5}(Na_{0.5}K_{0.5})_{0.5}TiO_3$ ceramics have been synthesized by solid state reaction technique and their dielectric (including relaxor behavior) and piezoelectric properties have been studied as a function of Sb-doping concentration. The dielectric constant was found to increase with moderate Sb-doping till 2 wt.%. A similar trend is observed for its transition and depolarization temperature. However, a further increase in doping concentration is found to deteriorate its structural, dielectric, piezoelectric and ferroelectric properties. The optimum doping concentration of Sb in BNKT, in order to enhance its various properties, is found to be in the range of 1–2 wt.%. A significant increase in its depolarization temperature (which restricts its application due to ferroelectric to anti-ferroelectric phase transition) has been achieved enhancing its application range. The d_{33} value as high as 115, 121, 129 and 100 pC/N was obtained for pure, 1 wt.%, 2 wt.% and 4 wt.% Sb-doped BNKT ceramics, respectively. The various results show that an optimum doping of 1–2 wt.% Sb improves its performance and makes it a promising candidate for various piezoelectric application in a wide temperature range.

Acknowledgements

We are thankful for the financial support received form the Department of Science & Technology through the Project "Synthesis of High Performance Piezoelectric Ceramic & Crystals for Device Fabrication (SERC Sanction No. 100/(IFD)/1637)". K. Kumar is thankful to UGC for research fellowship in 'Science for Meritorious Students'. B.K. Singh and M.K. Gupta are thankful to DST for Senior Research Fellow position.

References

[1] B. Jaffe, W.R. Cook, H. Jaffe, Piezoelectric Ceramics, Academic Press, London, 1971.
[2] K. Uchinoin, Present status of piezoelectric/electrostrictive actuators and remaining problems, in: H.L. Tuller (Ed.), Piezoelectric Actuators and Ultrasonic Motors, Kluwer Academic Publishers, Boston, 1997 (Chapter 10).
[3] G.H. Haertling, Ferroelectric ceramics: history and technology, J. Am. Ceram. Soc. 82 (1999) 797–818.
[4] J. Moulson, J.M. Herbert, Electroceramics, John Wiley & Sons Ltd., New York, 2003.
[5] X. Wang, H. Lai-Wa Chan, C.L. Choy, $(Bi_{1/2}Na_{1/2})TiO_3$–$Ba(Cu_{1/2}W_{1/2})O_3$ lead-free piezoelectric ceramics, J. Am. Ceram. Soc. 86 (2003) 1809–1811.
[6] D.Q. Xiao, D.M. Lin, J.G. Zhu, P. Yu, Investigation on the design and synthesis of new systems of BNT-based lead-free piezoelectric ceramics, J. Electroceram. 16 (2006) 271–275.
[7] J.R. Gomah-Pettry, S. Saıd, P. Marchet, J.P. Mercurio, Sodium-bismuth titanate based lead-free ferroelectric materials, J. Eur. Ceram. Soc. 24 (2004) 1165–1169.

[8] Z. Yang, Y. Hou, B. Liu, L. Wei, Structure and electrical properties of Nd_2O_3-doped $0.82Bi_{0.5}Na_{0.5}TiO_3$–$0.18Bi_{0.5}K_{0.5}TiO_3$ ceramics, Ceram. Int. 35 (2009) 1423–1427.
[9] D. Lin, D. Xiao, J. Zhu, P. Yu, Piezoelectric and ferroelectric properties of $[Bi_{0.5}(Na_{1-x-y}K_xLi_y)_{0.5}]TiO_3$ lead-free piezoelectric ceramics, Appl. Phys. Lett. 88 (2006) 62901–62903.
[10] Y. Li, W. Chen, Q. Xu, J. Zhou, Y. Wang, H. Sun, Piezoelectric and dielectric properties of CeO_2-doped $Bi_{0.5}Na_{0.44}K_{0.06}TiO_3$ lead-free ceramics, Ceram. Int. 33 (2007) 95–99.
[11] Y. Li, W. Chen, J. Zhou, Q. Xu, H. Sun, M. Liao, Dielectric and ferroelectric properties of lead-free $Na_{0.5}Bi_{0.5}TiO_3$–$K_{0.5}Bi_{0.5}TiO_3$ ferroelectric ceramics, Ceram. Int. 31 (2005) 139–142.
[12] T. Takenaka, H. Nagata, Current status and prospects of lead-free piezoelectric ceramics, J. Eur. Ceram. Soc. 25 (2005) 2693–2700.
[13] K. Fuse, T. Kimura, Effect of particle sizes of starting materials on microstructure development in textured $Bi_{0.5}(Na_{0.5}K_{0.5})_{0.5}TiO_3$, J. Am. Ceram. Soc. 89 (2006) 1957–1964.
[14] S. Zhao, G. Li, A. Ding, T. Wang, Q. Yin, Ferroelectric and piezoelectric properties of $(Na,K)_{0.5}Bi_{0.5}TiO_3$ lead free ceramics, J. Phys. D: Appl. Phys. 39 (2006) 2277–2281.
[15] X. Yi, H. Chen, W. Cao, M. Zhao, D. Yang, G. Ma, C. Yang, J. Han, Flux growth and characterization of lead-free piezoelectric single crystal $[Bi_{0.5}(Na_{1-x}K_x)_{0.5}]TiO_3$, J. Cryst. Growth 281 (2005) 364–369.
[16] S.E. Park, S.J. Chung, I.T. Kim, Ferroic phase transitions in $(Na_{1/2}Bi_{1/2})TiO_3$ crystals, J. Am. Ceram. Soc. 79 (1996) 1290–1296.
[17] C.S. Tu, I.G. Siny, V.H. Schmidt, Sequence of dielectric anomalies and high temperature relaxation behavior in $Na_{1/2}Bi_{1/2}TiO_3$, Phys. Rev. B 49 (1994) 11550–11559.
[18] G.A. Smolenskii, J. Phys. Soc. Jpn. 28 (1970) 26.
[19] B.K. Singh, K. Kumar, N. Sinha, B. Kumar, Flux growth and low temperature dielectric relaxation in piezoelectric $Pb[(Zn_{1/3}Nb_{2/3})_{0.91}Ti_{0.09}]O_3$ single crystals, Crys. Resh. Technol. 44 (2009) 915–919.
[20] A.K. Jonscher, Dielectric Relaxation in Solids, Chelsea Dielectric Press, London, 1983.
[21] H. Halliyal, U. Kumar, R.E. Newnham, L.E. Cross, Stabilization of the perovskite phase and dielectric properties of ceramics in the $Pb(Zn_{1/3}Nb_{2/3})O_3$–$BaTiO_3$ system, Am. Ceram. Soc. Bull. 66 (1987) 671–676.
[22] N. Vittayakorn, G. Rujijanagul, X. Tan, M.A. Marquardt, D.P. Cann, The morphotropic phase boundary and dielectric properties of the xPb$(Zr_{1/2}Ti_{1/2})O_3$–$(1-x)Pb(Ni_{1/3}Nb_{2/3})O_3$ perovskite solid solution, J. Appl. Phys. 96 (2004) 5103–5110.
[23] E.R. Leite, A.M. Scotch, A. Khan, T. Li, H.M. Chan, M.P. Harmer, S.F. Liu, S.E. Park, Chemical heterogeneity in PMN–35PT ceramics and effects on dielectric and piezoelectric properties, J. Am. Ceram. Soc. 85 (2002) 3018–3024.
[24] G.H. Haertling, W.J. Zimmer, Am. Ceram. Soc. Bull. 45 (1966) 1084.